

THE INTERNATIONAL JOURNAL OF SCIENCE & TECHNOLEDGE

ZnO Doped with Alkali Metals Serving for Optoelectronic Applications

R. Krithiga

Condensed Matter Laboratory, Department of Physics, Madras Institute of Technology
Anna University, Chennai, Tamilnadu, India

S. Sankar

Condensed Matter Laboratory, Department of Physics, Madras Institute of Technology
Anna University, Chennai, Tamilnadu, India

G. Subhashree

Condensed Matter Laboratory, Department of Physics, Madras Institute of Technology
Anna University, Chennai, Tamilnadu, India

Abstract:

A nitrate-glycine route combustion synthesis of ZnO and ZnO doped with Li, Na, K and is précised here along with the structural and optical properties. The XRD patterns of the samples clearly indicate the wurtzite hexagonal structure of the samples. Due to the difference in the ionic radii of the dopants, a minor variation is observed in the lattice constants. The undoped ZnO has the smallest grain size; ZnO: Li has the second smallest grain size followed by ZnO: Na and then ZnO: K. The UV-Vis-NIR spectra of the samples are utilized to calculate the photon band gap. The band gap shows a considerable red shift for all dopants. The fluorescence spectra of the samples have a weak UV emission and a dominant emission in visible region. The visible emission shows a blue shift whereas the UV emission shows a red shift down the alkali group. The observed tuning capability of the band gap and the photo luminescent properties in the materials could greatly find applications in optoelectronic industry.

Keywords: ZnO, Combustion synthesis, X-Ray diffraction, UV-Vis-NIR, Fluorescence spectra

1. Introduction

ZnO has progressed as one of the significant materials owing to interesting dielectric, semiconducting, optical, photo electrochemical, and electrical properties. ZnO with a wide band gap of 3.2eV and exciton binding energy of 60 meV has very eclectic applications which includes transparent conducting electrodes of solar cells, flat panel displays, surface acoustic devices, UV lasers and biological sensors [1-5]. The characteristics of ZnO rests on its size and the synthesis route. Nano-scale ZnO retain different physical and chemical properties compared to bulk ZnO. The synthesis of nano size ZnO powder has been carried out by diverse approaches such as sol-gel, co-precipitation, auto-combustion, and hydrothermal methods [6-10]. The sol-gel auto-combustion is relatively one of the new methods for synthesizing nano ZnO powder and there is a higher degree of atomic homogeneity when dopants are added. ZnO behaves differently with different dopants. The stratagem of doping ZnO in recent works speaks the expectations and interests for the material. To make ZnO a semi-magnetic material it has been doped with transition elements [11]. The optical property is tailored by doping lanthanides [12]. Recently the elements from alkali group and pnictogen group are also doped even they are less soluble [13, 14]. The solubility of dopants are enhanced by codoping of lanthanides with alkali elements and pnictogens to have altered electrical and optical properties [15]. In the present work the alkali elements lithium, sodium and potassium are codoped with ZnO with a view to investigate the effects of monovalent impurities on the optical properties. The synthesis is carried out by simple sol-gel auto combustion method.

2. Experimental Details

The ZnO doped with 2% Li, Na and K are synthesized by dissolving the stoichiometric amounts of zinc nitrate, lithium nitrate/ sodium nitrate/ potassium nitrate and glycine in distilled water to get an aqueous solution. The glycine acts as fuel for the reaction involving combustion. Glycine is chosen as fuel because the combustion enthalpy is more negative when compared to urea or citric acid. The aqueous solution taken in a beaker is stirred and heated for 1 h to ensure better homogeneity. After 1 h the solution becomes a gel with minimum water content. The gel then swells, foams and rises to undergo a self-propagating auto combustion reaction leaving fine powders of ZnO: Li/ Na/ K ultimately. The powders are heated to 500°C for 3 h for the leftover nitrates to react. The as-synthesized powders are ground well for 1 h to have fine texture and preserved for studies. The powders are characterized by using an X-Ray diffractometer (XRD) (PAnalytical X'pert PRO) and scanning electron microscope (SEM) (Bruker) for the structural properties. The optical properties are studied using Ultraviolet-Visible-Near Infra-Red spectrophotometer (UV-Vis-NIR) (LabIndia UV 3000 +) and spectrofluorimeter (JY Fluorolog-3-11).

3. Results and Discussion

3.1. Structural analysis

3.1.1. XRD analysis

The structural properties of the samples are analyzed from the XRD pattern obtained. The grain sizes are determined from the XRD pattern using the Debye-Scherrer relation [16] given by $G = \frac{K\lambda}{\beta \cos\theta}$, where K is known as the shape factor (takes as 0.9 for Gaussian like peak profiles), λ is the x-ray wavelength (1.5406 Å for Cu-K α), β is full width at half maximum in radian and θ is the Bragg angle of diffraction. The lattice parameters are calculated by the relation $\sin^2\theta = \frac{\lambda^2}{4a^2} \left[\frac{4}{3}(h^2 + k^2 + lk) + \frac{l^2}{c^2} \right]$ where 'a' and 'c' are lattice parameters. The XRD pattern shown in FIG.1, contains the standard peaks of ZnO (JCPDS 36-1451) indexed as (100), (002), (101), (102), (110), (103), (200), (112) and (201) confirming the hexagonal wurtzite structure. The XRD patterns show no additional peaks for doped ones when compared to ZnO indicating the proper incorporation of alkali ions in ZnO lattice. The estimated values of particle size and lattice constant are given in Table 1. It is seen from the Table 1 that the lattice parameters 'a' remains constant but 'c' changes with the alkali dopant which is understood as the alkali substitution along 'c' axis.

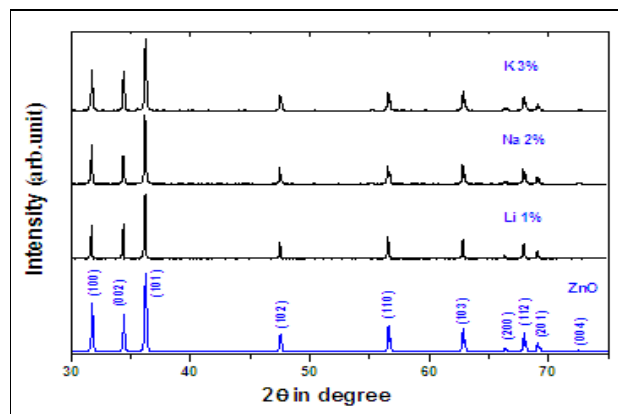


Figure 1: XRD Patterns of ZnO, ZnO: Li, ZnO: Na and ZnO: K

3.2. Optical Study

3.2.1. UV-Vis-NIR Analysis

The FIG.2 shows the optical absorbance spectra of ZnO and alkali doped ZnO. The band gap of the samples are estimated from the absorbance by applying Tauc model [17] and Davis and Mott model [18] in the high absorption region. The variation of $(\alpha h\nu)^2$ with respect to $h\nu$ is shown in FIG.8. The band gap energies are obtained from the plot by extrapolating the linear portion to the photon energy axis where $\alpha=0$. The band gap show a red shift that confirms the incorporation of sodium atoms into ZnO lattice.

It is remarkable to note that for the Na dopant, the band gap decreases drastically to 2.87 eV. The K dopant and Li dopant shrink the band gap to 3.16 and 3.18 respectively. This is decrease in the photon band gap may be attributed to the effect of grain size. This 'bowing' of the curve in the band gap is due to the formation of donor levels inside the band gap due replaced Zn atoms present in the lattice by alkali atoms. This decrease in band gap of Na doped ZnO is attributed to the intermediate levels formed by oxygen vacancy at 190 meV from the conduction band edge [19].

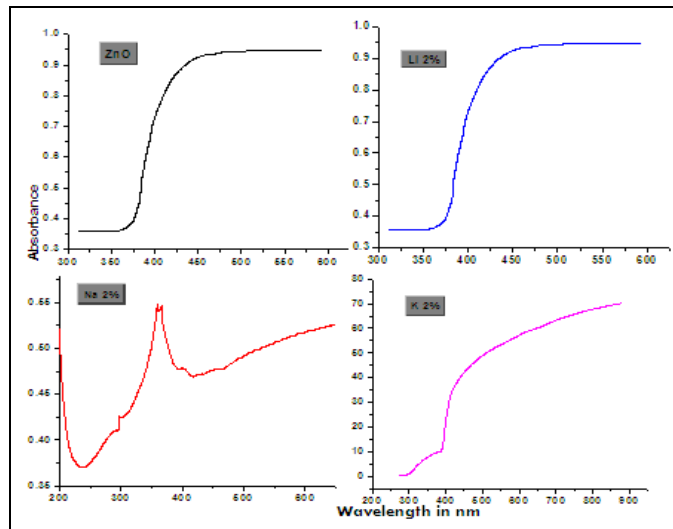


Figure 2: UV-Vis-NIR spectra of ZnO, ZnO: Li, ZnO: Na, ZnO: K samples

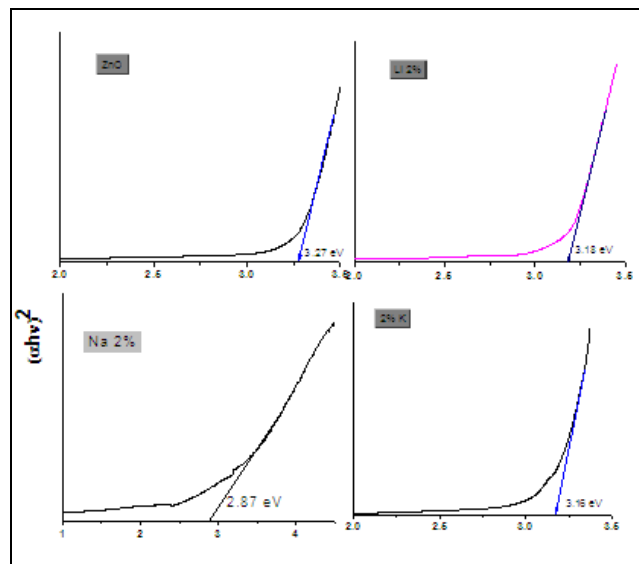


Figure 3: Tauc plot of ZnO, ZnO: Li, ZnO: Na and ZnO: K

3.2.2. Photoluminescence

The photoluminescence properties of ZnO and alkali doped ZnO were characterized by spectrofluorometer at room temperature. The emission source is a xenon lamp. FIG. 4 shows the PL spectra of the samples excited at the wavelength of 290 nm for detecting PL peaks in the range 325 – 620 nm. It is seen that the intensity of UV emission lessens for alkali doped ZnO whereas the VIS intensity strengthens for alkali doped ZnO. The Li doped sample emit a strong green luminescence at 489 nm. The Na doped ZnO exhibits a violet emission centered at 417 nm and the K doped ZnO emits blue light around 420 nm. The decrease of UV intensities is attributed to the increase in the probability of non-radiative recombination [20] and decrease of crystallinity. For the doped ZnO, the alkali dopants substitutes for Zn atoms in ZnO lattice thus forming Zn interstitials. The transition of electrons from Zn_i to the VB is responsible for blue emission and violet emissions. The neutral Zn atom in interstitial (Zn^0) ejects an electron (e^-) when irradiated by UV photons i.e. $Zn^0 \rightarrow Zn^+ + e^-$. Thus ejected electron is trapped in oxygen vacancy to become V_o^* . Now Zn^0 acts as a hole center whereas V_o^* acts as electron center. The recombination of these two causes the green emission of Li doped ZnO [21].

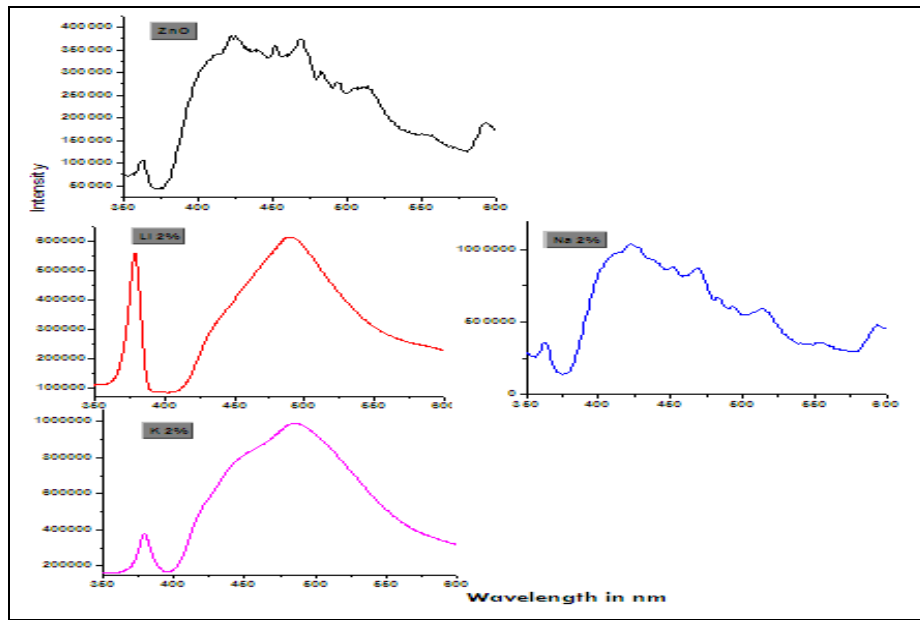


Figure 4: PL spectrum of ZnO, ZnO: Li, ZnO: Na and ZnO: K

4. Conclusion

Alkali doped ZnO are synthesized by sol-gel auto combustion method. The structural and the optical properties are reported here. The substitution of alkali ions for Zn ions is well observed in the results. The hexagonal wurtzite structure is confirmed from XRD studies. The grain size increases for all alkali dopants. The UV analysis estimates the band gap and predicts a red shift in the energy gap. The UV emission intensity decreases down the group and VIS emission intensifies down the group. The PL analysis confirms oxygen vacancy and Zn_i that has reduced the band gap considerably. Ultimately the effect of the alkali dopants is to enhance the PL emission in visible region and UV region making the materials more suitable for optoelectronic applications.

5. Acknowledgments

The author R. Krithiga is grateful to Anna University for funding this research under ANNA CENTENARY RESEARCH FELLOWSHIP scheme. The authors acknowledge SRM University and SAIF- IIT Chennai for permitting to use the characterization facilities.

6. References

1. P. Zu, Z.K. Tang, G.K. Wong, M. Kawasaki, H. Ohtomo, H. Koinuma, Y. Segawa, *Solid State Commun.* 103, 459 (1997)
2. D.M. Bangall, Y.G. Chen, Z. Zhu, T. Yao, *Appl. Phys. Lett.* 70, 2230 (1997)
3. Y.C. Kong, D.P. Yu, B. Zhang, W.Fang, S.Q. Feng, *Appl. Phys. Lett.* 78, 407 (2001)
4. Y. Li, G.W. Meng, L.D. Zhang, F. Philip, *Appl. Phys. Lett.* 76, 2011 (2000)
5. K. Omichi, K. Kaiya, N. Takahashi, T. Nakamura, S. Okamoto, H. Yamamoto, *J. Mater. Chem.* 11, 262 (2001)
6. S. Senthilkumaar, K. Rajendran, S. Banerjee, T.K. Chini, V. Sengodan, *Mater. Sci. Semicond. Process.* 11, 7 (2008)
7. A.E. Jiménez-González, Jose A. Soto Urueta, R. Suárez-Parra, *J. Cryst. Growth* 192, 431 (1998)
8. R.S. Yadav, A.C. Pandey, S.S. Sanjay, *Chalcogenide Lett.* 6, 234 (2009)
9. Cheng-Shiung Lin, Chyi-Ching Hwang, Wei-Hua Lee, Wei-Yin Tong, *Mater. Sci. Eng. B* 140, 32 (2007)
10. Nuengruethai Ekthammathat, Titipun Thongtem, Anukorn Phuruangrat, Somchai Thongtem, *Superlattices Microstruct.* (2013) doi: 10.1016/j.spmi.2012.10.013
11. F. Pan, C. Song, X.J. Liu, Y.C. Yang, F. Zeng, *Mater. Sci. Eng.: R* (2008) doi: 10.1016/j.mserr.2008.04.002
12. Li Ji-le, Guo-hua Chen, Chang-lai Yuan, *Ceram. Int.* 39, 2235 (2013)
13. S.S. Lin, J.G. Lu, Z.Z. Ye, H.P. He, X.Q. Gu, L.X. Chen, J.Y. Huang, B.H. Zhao, *Solid State Commun.* 148, 26 (2008)
14. Y.F. Lu, Z.Z. Ye, Y.J. Zeng, L.P. Zhu, J.Y. Huang, B.H. Zhao, *Solid-State Electron.* 54, 733 (2010)
15. Honglin Li, Zhong Zhang, Jinzhao Huang, Ruxi Liu, Qingbao Wang, *J. Alloys. Compd.* 550, 526 (2013)
16. B.D. Cullity, *Elements of X-ray Diffractions*, Addison-Wesley Reading, MA. 1978
17. J. Tauc, *Amorphous and Liquid Semiconductors*, Plenum, London, 1974
18. E.A. David, N.F. Mott, *Philos. Mag.* 22, 903 (1970)
19. Y. S. Yu, G.Y. Kim, B.H. Min, S.C. Kim *J. Eur. Ceram. Soc.* 24, 1867 (2004)
20. Yu-Chih Tseng, Yow-Jon Lin, Hsing-Cheng Chang, Ya-Hui Chen, Chia-Jyi Liu, Yi-Yan Zou, *J. of Lumin.* 132, 1898 (2012)
21. R. Krithiga, S. Sankar, G. Subhashree, *J. Mater. Sci: Mater. Electron.* 25, 109 (2014)